JOURNAL OF VIROLOGY, Apr. 2006, p. 3541–3548 Vol. 80, No. 7
0022-538X/06/$08.00+0 doi:10.1128/JVI.80.7.3541–3548.2006

UL26-Deficient Human Cytomegalovirus Produces Virions with Hypophosphorylated pp28 Tegument Protein That Is Unstable within Newly Infected Cells

Joshua Munger, Dong Yu,† and Thomas Shenk*

Department of Molecular Biology, Princeton University, Princeton, New Jersey 08544-1014

Received 19 September 2005/Accepted 19 January 2006

The human cytomegalovirus UL26 open reading frame encodes proteins of 21 and 27 kDa that result from the use of two different in-frame initiation codons. The UL26 protein is a constituent of the virion and thus is delivered to cells upon viral entry. We have characterized a mutant of human cytomegalovirus in which the UL26 open reading frame has been deleted. The UL26 deletion mutant has a profound growth defect, the magnitude of which is dependent on the multiplicity of infection. Two very early defects were discovered. First, even though they were present in normal amounts within mutant virions, the UL99-coded pp28 and UL83-coded pp65 tegument proteins were present in reduced amounts at the earliest times assayed within newly infected cells; second, there was a delay in immediate-early mRNA and protein accumulation. Further analysis revealed that although wild-type levels of the pp28 tegument protein were present in UL26 deletion mutant virions, the protein was hypophosphorylated. We conclude that the UL26 protein influences the normal phosphorylation of at least pp28 in virions and possibly additional tegument proteins. We propose that the hypophosphorylation of tegument proteins causes their destabilization within newly infected cells, perhaps disrupting the normal detegumentation process and leading to a delay in the onset of immediate-early gene expression.

Human cytomegalovirus (HCMV), the prototypic betaherpesvirus, is a leading cause of congenital infection which can result in multiple-organ-system abnormalities, with damage to the auditory system occurring in the majority of symptomatic newborns (9). HCMV infection also posses a serious health risk to immunosuppressed individuals, such as cancer patients receiving immunosuppressive chemotherapy, transplant recipients, and AIDS patients (9). Recently, HCMV infection also has been implicated as a cofactor in atherosclerosis and restenosis following coronary angioplasty (9).

The ~240-kb HCMV genome encodes >200 open reading frames (ORFs). HCMV is an enveloped virus: its genome is encased within a capsid, and a protein layer called the tegument resides between the capsid and envelope. The tegument proteins (3, 22), which are unique to herpesviruses, are delivered to cells upon infection and can act before the onset of viral gene expression to help initiate a productive infection. Examples of tegument proteins include the UL69 protein, which blocks cell cycle progression in late G_1 (14); the UL82-coded pp71, which acts as a transcriptional transactivator (10) and stimulates quiescent cells to enter the mitotic cycle (14); the UL83-coded pp65 and IRS1 plus TRS1 proteins, which antagonize aspects of the cellular antiviral response (1, 5, 6); and the UL99-coded pp28, which mediates the cytoplasmic envelopment of tegument capsids (20).

The UL26 protein (pUL26) is present in the tegument of the virion (3, 21, 22). It is expressed with early kinetics, and synthesis of the protein initiates at one of two start codons, yielding either a 21- or 27-kDa product. A segment of the UL26 coding region was isolated in an activator trap assay, arguing that the protein includes a transcriptional activator domain (21).

We analyzed the function of pUL26 by examining the phenotype of a UL26 deletion mutant. The mutant exhibited a strong growth defect in fibroblasts. Its virions contained normal levels of the tegument proteins that were assayed, but at least one of them, UL99-coded pp28, was hypophosphorylated. A reduced level of hypophosphorylated pp28 was evident in newly infected cells, suggesting that it is unstable, and there was a marked delay in the accumulation of IE1 mRNA and protein.

MATERIALS AND METHODS

Biological reagents. Primary human foreskin fibroblasts (HFFs; passages 6 to 15) were cultured in Dulbecco's modified Eagle medium containing 7.5% fetal calf serum. AD*wt* is the AD169 HCMV laboratory strain (18). BAD*sub*UL26, which was derived from a bacterial artificial chromosome (BAC) clone of AD169 termed pAD/Cre (24), was described previously (23). In this mutant, the UL26 ORF has been replaced with a transposon that carries a marker cassette encoding kanamycin resistance and β-galactosidase in bacterial cells and green fluorescent protein in mammalian cells. A repaired, wild-type revertant of BAD*sub*UL26, termed BAD*rev*UL26, was created by allelic exchange (24). Briefly, the UL26 ORF with approximately 100 bp of upstream and 100 bp of downstream flanking sequences was cloned into the pGS284 shuttle vector. Allelic exchange was performed by using the BAC clone of BAD*sub*UL26, termed BAC-BAD*sub*UL26 (23), to restore the UL26 ORF and simultaneously delete the kanamycin resistance and β-galactosidase markers, thus facilitating screening. The BAD*rev*UL26 virus was reconstituted by electroporation of HFF cells with the modified BAC. Wild-type and mutant HCMVs were propagated, and the titers were determined by plaque assay on HFFs.

HFFs expressing pUL26 were generated by infection with a recombinant retrovirus. To generate the retrovirus, the UL26 ORF was amplified from pAD/Cre (24), using the following primers: AGT TTG AGC GAA TTC ATG TAC GCC GTT TTC and ATT TTG CCC GGG CAA CAG CGC TGA TGG. The PCR-generated product was cloned into the Xma/EcoR1 sites of pBluescript, and two short DNA fragments (CCG GGG ACT ACA AAG ACC ATG ACG GTG ATT ACCA AGG ATG ACG ATG ACT AAGC and GGC CGC TTA

* Corresponding author. Mailing address: Department of Molecular Biology, Princeton University, Princeton, NJ 08544-1014. Phone: (609) 258-5992. Fax: (609) 258-1704. E-mail: tshenk@princeton.edu.

† Present address: Department of Molecular Microbiology, Washington University School of Medicine, St. Louis, MO 63110.

GTC ATC GTC ATC CTT GTA ATC ACC GTC ATG GTC TTT GTA GTCC), containing two Flag-tag epitopes, were then cloned in-frame at the C terminus of the UL26 coding region to generate pBlueUL26F. The UL26-Flag fragment was subcloned from pBlueUL26F into pLPCX (Clontech), creating pLPCX-26F, and a retrovirus stock, retro-26F, was prepared by transfecting this plasmid into Phoenix Ampho cells (11). HFFs were infected with retro-26F to generate a population of FLAG-tagged pUL26 (pUL26F)-expressing cells.

To produce a UL26-specific monoclonal antibody, the UL26-Flag DNA segment from pBlueUL26F was subcloned into pGex4T1 to create pGex26F. A glutathione *S*-transferase (GST) fusion protein, GST-26F, was then produced by transfection of *Escherichia coli* BL-21 with pGex26F. The resulting fusion protein was affinity purified on glutathione Sepharose as recommended by the manufacturer (Amersham Pharmacia Biotech). Purified protein was used to immunize 5-week-old BALB/c mice. Mice were boosted with GST-26F twice and screened for seroconversion, and spleens were harvested for fusion. Hybridomas secreting antibody to pUL26 were screened, selected, and amplified. In addition to pUL26-specific antibody, monoclonal antibodies to the following viral proteins were employed: IRS1 (1B4 [17]), TRS1 (9A1 [17]) UL99-coded pp28 (10B4-29 [20]), UL83-coded pp65 (8F5 [16]), UL123-coded IE1 (1B12 [A. Marchini, P. Robinson, and T. Shenk, unpublished]), pUL44 (10D8; Virusys), and the UL86-coded major and UL85-coded minor capsid proteins (kind gifts from W. Gibson, Johns Hopkins).

Analysis of viral DNA, RNA, and protein. Viral DNA accumulation was monitored by slot blot assay. Cells were scraped, pelleted by low-speed centrifugation, washed with phosphate-buffered saline (PBS), and lysed in buffer containing 100 mM NaCl, 10 mM Tris (pH 8.0), 25 mM EDTA, 0.5% sodium dodecyl sulfate (SDS), and 0.1 mg of proteinase K/ml. After incubation for 3 h at 55°C, DNA was extracted with phenol-chloroform and precipitated with ethanol. Aliquots (1 μg) were transferred to a nylon membrane using a slot blot apparatus. Immobilized viral DNA was hybridized to either a ^{32}P-labeled random-primed probe from pAD/Cre DNA or a digoxigenin-labeled probe from a PCR-generated fragment of the UL36 gene generated using a digoxigenin probe synthesis kit (Roche).

For the analysis of IE1 mRNA, total RNA was prepared from infected cells, using Trizol as recommended by the manufacturer (Invitrogen). Equivalent amounts of RNA was then glyoxalated, subjected to 1.0% agarose gel electrophoresis, and transferred to a nylon membrane (2). Methylene blue staining of the membrane was used to ensure equivalent RNA loading and transfer. A ^{32}P-labeled probe specific for IE1 was generated by random-primed synthesis from an IE1 plasmid (12). Northern hybridization was performed as described elsewhere (2).

Protein accumulation was assayed by Western blotting. Cells were scraped, pelleted by low-speed centrifugation, washed with PBS and solubilized in cellular lysis solution in buffer containing 150 mM KCl, 10 mM HEPES, 1% NP-40, 0.5% deoxycholate, 0.1% SDS, 10 μg/ml phenylmethylsulfonyl fluoride, 1 μg/ml pepstatin, 10 mM NaF, and 100 μM sodium orthovanadate. After 10 min on wet ice, lysates were centrifuged at 14,000 × *g* for 10 min. The protein concentration of supernatant fluids was determined by using the Bio-Rad assay, according to the directions of the manufacturer. Equivalent amounts of protein (10 to 60 μg) were denatured in disruption buffer (50 mM Tris [pH 7.0], 2% SDS, 5% 2-mercaptoethanol, and 2.75% sucrose), subjected to electrophoresis in an SDS-containing 11% polyacrylamide gel, and transferred to a nitrocellulose sheet. Blots were then stained with Ponceau S to ensure equivalent protein loading and transfer, blocked by treatment with 5% milk, and reacted with primary antibody. Protein bands were visualized through enhanced chemiluminescent detection, according to the instructions of the manufacturer (Pierce).

To produce partially purified virions for the analysis of their constituent proteins, virus stocks were first clarified by low-speed centrifugation and then centrifuged through a sorbitol cushion at 55,000 × *g* for 1 h. The virion pellet was then resuspended in buffer containing 50 mM Tris, pH 7.4, and 100 mM NaCl and purified by centrifugation through a glycerol tartrate gradient as previously described (3). Bands containing virions were collected and virions were repelleted by centrifugation through a sorbitol cushion at 55,000 × *g* for 1 h and resuspended in either cellular lysis solution (described above), 2-D rehydration buffer (2% CHAPS, 8 M urea and 0.5% 3-10 IPG buffer) (Amersham Pharmacia Biotech) or λ phosphatase buffer (50 mM Tris [pH 7.5], 0.1 mM EDTA, 5 mM dithiothreitol, 0.01% Brig 35, 2 mM $MnCl_2$).

For two-dimensional (2-D) gel analysis of virion proteins, virions were resuspended in 250 μl of 2-D rehydration buffer, centrifuged to pellet insoluble material, loaded onto a 13-cm Immobiline Drystrep isoelectric-focusing gel (pH 7 to 10) (Amersham Biotech), and proteins were separated using the IPGphor isoelectric-focusing system as directed by the manufacturer (Amersham). After focusing, gels were equilibrated for 15 min in 50 mM Tris (pH 8.8), 6 M urea, 30% glycerol, 2% SDS, and 10 mg/ml dithiothreitol, then the proteins in the gel were subjected to electrophoresis in the second dimension through an SDS-containing 11% polyacrylamide gel, and proteins were identified by Western blot assay, as described above.

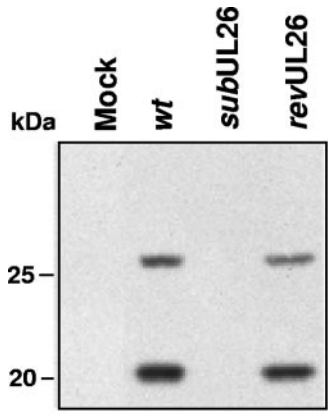

FIG. 1. Accumulation of pUL26 protein in cells infected with wild-type or pUL26-deficient deletion mutant HCMV. Replicate cultures of fibroblasts were infected at a multiplicity of 3.0 PFU/cell with AD*wt*, BAD*sub*UL26, or BAD*rev*UL26. Cells were harvested 48 h postinfection and processed for Western blotting using a pUL26-specific monoclonal antibody.

For 2-D gel analysis of phosphatase-treated virions, partially purified virions were resuspended in λ phosphatase buffer with or without phosphatase inhibitors (10 mM NaF, 100 μM sodium orthovanadate). Virions were then incubated at 30°C with or without 800 units of λ protein phosphatase (New England Biolabs) for 1 h, then the sample volume was brought up to 250 μl with 2-D rehydration buffer and samples were processed for 2-D gel analysis as described above.

For immunofluorescence, fibroblasts were grown on glass coverslips. At various times postinfection, cells were washed twice with PBS, fixed with 2% paraformaldehyde in PBS for 20 min, washed twice with PBS, and permeablized with 0.1% TX-100 for 15 min when staining with pp28-specific antibody or permeabilized with 0.1% TX-100 and 0.1% SDS for 15 min when staining with pUL26-specific antibody. Cells were subsequently washed twice with PBS containing 0.05% Tween-20 and blocked by incubation for 1 h in PBS containing 2% bovine serum albumin and 0.05% Tween-20. Cells were incubated with primary antibody diluted in PBS plus 0.05% Tween-20 for 1 h, washed in the same buffer lacking antibody three times, incubated with fluorochrome-conjugated anti-mouse secondary antibody and DAPI (4′,6′-diamidino-2-phenylindole) as a nuclear stain for 1 h, and washed again three times. Coverslips were mounted in slow-fade solution (Molecular Probes) and analyzed by confocal microscopy.

RESULTS

Localization of the UL26 protein. A mouse monoclonal antibody directed against pUL26 was produced. To test its specificity, fibroblasts were mock infected or infected with AD*wt* (wild-type AD169), BAD*sub*UL26 (UL26-deficient mutant), or BAD*rev*UL26 (repaired mutant). At 48 h postinfection, cells were harvested, lysed, and analyzed by Western blotting. Two bands, with approximate molecular weights of 21 and 27 kDa, were present in the AD*wt*- and BAD*rev*UL26-infected cell lysates but not in the mock- or BAD*sub*UL26-infected cell lysates (Fig. 1). This result showed that the anti-pUL26 monoclonal antibody is specific, that BAD*sub*UL26 fails to produce detectable levels of pUL26 and that the repair of the UL26 locus in BAD*rev*UL26 restored pUL26 accumulation. Additionally, it confirmed the earlier demonstration by Stamminger et al. (15) that two forms of pUL26 are produced.

To determine the subcellular localization of pUL26, fibroblasts were infected with AD*wt*, fixed at various times, and

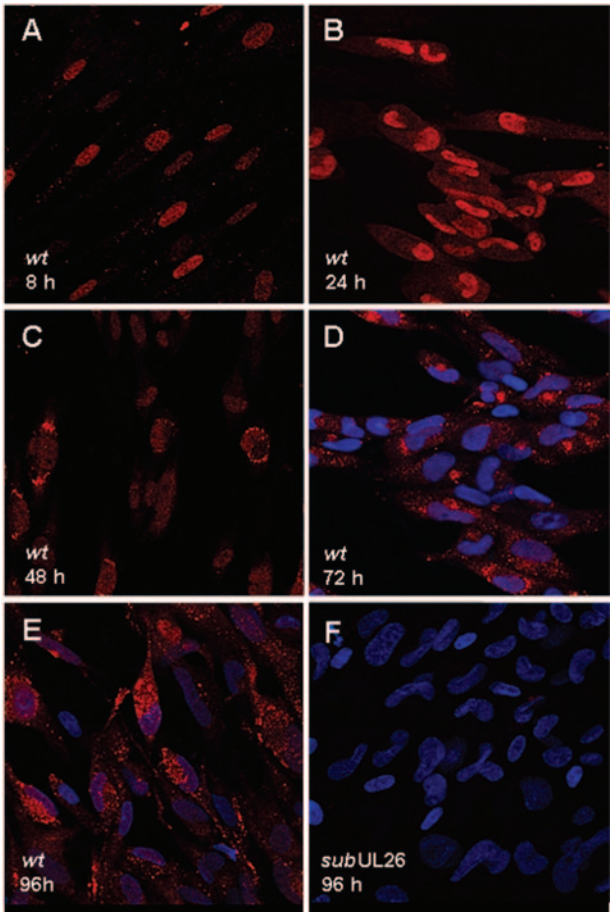

FIG. 2. Localization of pUL26 protein in cells infected with wild-type or a pUL26-deficient mutant of HCMV. Replicate cultures of fibroblasts cells were infected at a multiplicity of 3.0 PFU/cell with AD*wt* or BAD*sub*UL26 multiplicity of infection. Cells were fixed at the indicated time points and processed for immunofluorescence using a pUL26-specific monoclonal antibody.

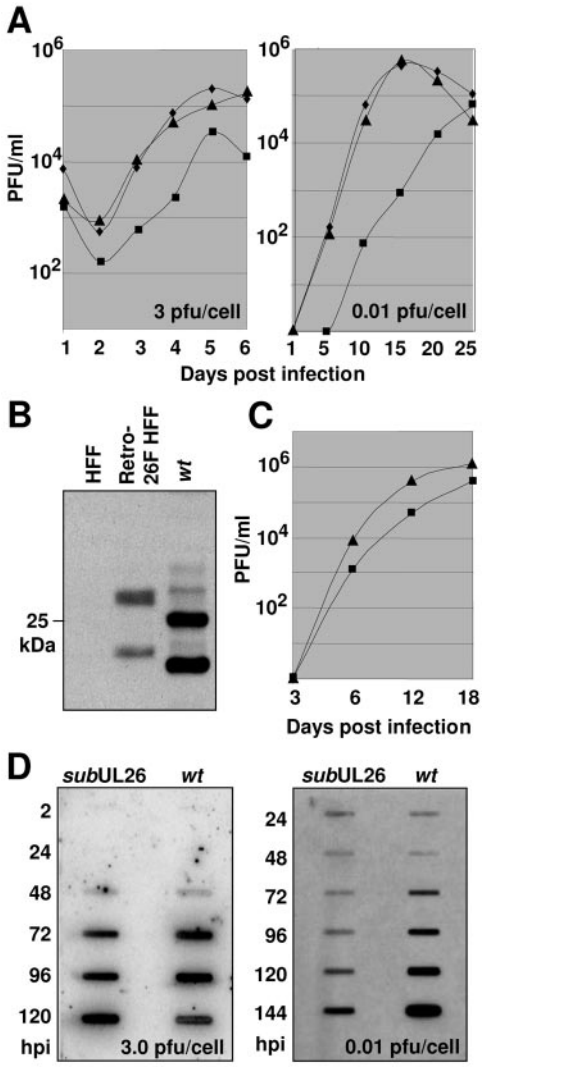

FIG. 3. Growth characteristics of wild-type and pUL26-deficient viruses. (A) Production of infectious progeny in fibroblast cultures. Replicate cultures were infected at a multiplicity of 3.0 or 0.01 PFU/cell with AD*wt* (▲), BAD*sub*UL26 (■), or BAD*rev*UL26 (◆). Cells were harvested at the indicated times, and infectious viral progeny was quantified by plaque assay on fibroblasts. (B) Mock-infected fibroblasts transduced with a retrovirus expressing pUL26 as well as mock- or AD*wt*-infected (multiplicity of 3.0 PFU/cell) nontransduced fibroblasts were harvested and processed for Western blotting using a pUL26-specific monoclonal antibody. (C) Production of infectious progeny in fibroblasts expressing pUL26. Replicate cultures of retrovirally transduced fibroblasts expressing pUL26 were infected at a multiplicity of 0.01 PFU/cell with AD*wt* (▲) or BAD*sub*UL26 (■). Cells were harvested at the indicated times and assayed for infectious viral progeny by plaque assay on fibroblasts. (D) Accumulation of viral DNA after infection with wild-type or UL26-deficient viruses. Replicate cultures of fibroblasts were infected at a multiplicity of 3.0 or 0.01 PFU/cell with AD*wt* or BAD*sub*UL26 and harvested at the indicated times. Total cellular DNA was assayed by slot blotting using an HCMV-specific probe.

processed for immunofluorescence with the pUL26-specific antibody (Fig. 2A to E). At 8 h postinfection, pUL26 was localized to numerous punctate structures in the nucleus. As the infection progressed (24 h), pUL26 fluorescence became more intense in the nucleus and was also detected in the cytoplasm. During the late phase of infection (48, 72, and 96 h), pUL26 was localized to a much lesser extent in the nucleus and increasingly at juxtanuclear virion assembly centers, similarly to other virion proteins (19). As expected, the BAD*sub*UL26 mutant failed to produce detectable pUL26 (Fig. 2F). The early nuclear localization of pUL26 during HCMV infection correlates with the reported transcriptional effect of pUL26 on the HCMV major immediate-early promoter (21), and its punctate juxtanuclear cytoplasmic localization agrees with the finding that the UL26 protein is incorporated into virus particles (3, 21, 22).

pUL26 is required to achieve a normal HCMV yield. We (23) and others (7) previously defined UL26 as an augmenting ORF, showing that a pUL26-deficient virus could replicate in fibroblasts but failed to produce a wild-type yield. To more thoroughly elucidate the impact of pUL26 on the kinetics and extent of HCMV replication, growth curves were performed. Fibroblasts were infected at a multiplicity of 3.0 or 0.01 PFU/cell with AD*wt*, BAD*sub*UL26, or BAD*rev*UL26, and the production of infectious virus was monitored as a function of time after infection by plaque assay. As shown in Fig. 3A, the

pUL26-deficient virus grew to a lesser extent than AD*wt* or BAD*rev*UL26, and the defect was more pronounced at the lower input multiplicity. After infection at 3 PFU/cell, BAD *sub*UL26 produced approximately 10-fold less progeny than the wild-type virus at all times assayed after 24 h, although the kinetics of virus production were similar (Fig. 3A, left panel). In contrast, after infection at 0.01 PFU/cell, BAD*sub*UL26 grew with much slower kinetics than AD*wt* or BAD*rev*UL26, initially exhibiting a delay in the production of infectious progeny (Fig. 3A, right panel). The wild-type and revertant viruses reached maximal yields on day 15, a time at which the mutant virus produced a 500-fold reduced yield. BAD*sub*UL26 generated a maximal yield on day 25, at which time it had produced a 10-fold lower yield than the maximum reached by wild-type viruses. By day 25, the wild-type-virus infectious titers had started to fall. In sum, deletion of the UL26 ORF resulted in a general replication defect that is kinetically exacerbated by infection at a low input multiplicity.

To determine if pUL26 supplied in *trans* could rescue the growth of the mutant, fibroblasts were transduced with a retrovirus expressing Flag-tagged pUL26. Expression of both pUL26 isoforms (21 and 27 kDa) was confirmed by Western blot assay (Fig. 3B); the retrovirally expressed Flag-tagged pUL26 migrated slightly slower than untagged pUL26 from AD*wt* infection. The replication of AD*wt* and BAD*sub*UL26 after infection at a multiplicity of 0.01 PFU/cell was then tested on the pUL26-expressing fibroblasts. The expression of pUL26 rescued the severe kinetic defect seen after infection of normal fibroblasts at a low input multiplicity (Fig. 3, compare panel A, right panel, to panel C); a >500-fold difference in peak yield of the wild type compared to mutant virus in normal fibroblasts was reduced to a <10-fold difference in pUL26-expressing fibroblasts. The remaining defect could result from the reduced pUL26 accumulation in the retrovirus-transduced fibroblasts, in comparison to HCMV-infected fibroblasts (Fig. 3B). Alternatively, the Flag tag on the pUL26 expressed from the recombinant retroviruses could negatively impact its activity. Nevertheless, the ability to completely restore the mutant virus replication defect by repairing the UL26 locus in BAD*rev*UL26 (Fig. 3A), coupled with the ability to compensate for the mutation in BAD*sub*UL26 by expression of pUL26 in *trans* (Fig. 3C), demonstrates that the phenotype observed in the mutant virus results from the loss of pUL26 expression.

Deletion of the UL26 ORF delays the onset of immediate early gene expression. To determine whether the BAD*sub*UL26 defect resides before or after the initiation of viral DNA replication, the kinetics of viral DNA accumulation was monitored. After infection of fibroblasts at a multiplicity of 3 PFU/cell, the mutant and wild-type viruses accumulated viral DNA similarly (Fig. 3D, left panel). In contrast, after infection at a lower input multiplicity (0.1 PFU/cell), the accumulation of BAD*sub*UL26 DNA was delayed (Fig. 3D, right panel). An increase over input levels of DNA was evident for the wild-type virus at 72 h postinfection, whereas the increase was not evident for BAD*sub*UL26 DNA until 120 h postinfection. Thus, the more modest defect observed after infection at a higher input multiplicity does not appear to strongly affect the kinetics of viral DNA replication, whereas the defect observed after infection at 0.1 PFU/cell negatively impacts infection either at or prior to DNA replication. These results support our finding

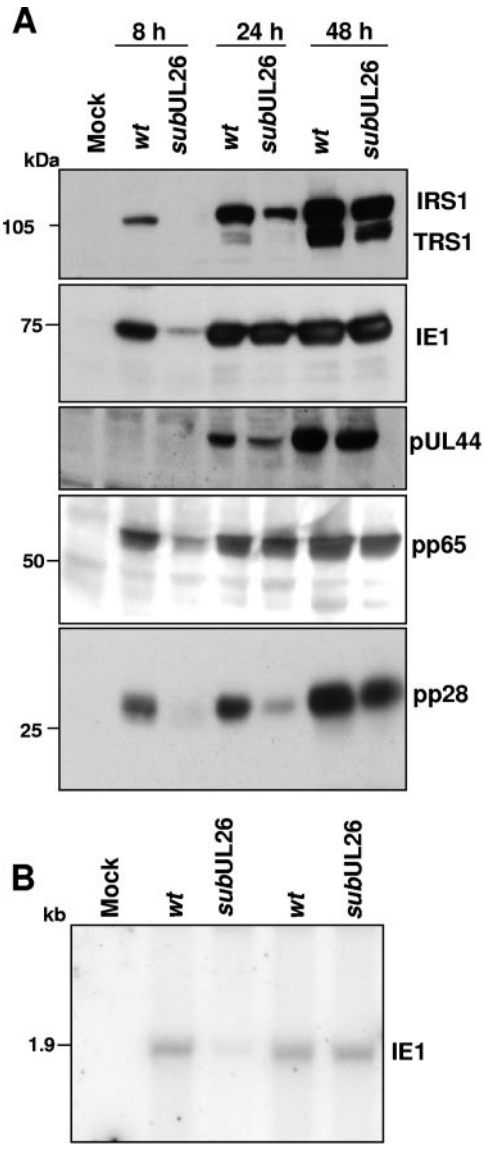

FIG. 4. Accumulation of viral proteins and mRNA in cells infected with wild type or a UL26-deficient mutant of HCMV. (A) Replicate cultures of fibroblasts were infected at a multiplicity of 3.0 PFU/cell with AD*wt* or BAD*sub*UL26. Cells were harvested at the indicated times and processed for Western blotting using antibodies directed toward pIRS1, pTRS1, IE1, pp65, pUL44, or pp28. (B) Replicate cultures of fibroblasts were infected at a multiplicity of 3.0 PFU/cell with AD*wt* or BAD*sub*UL26. Cells were harvested at the indicated times, and total mRNA was analyzed by Northern blot using a probe specific for IE1.

that the mutant exhibits a greater growth defect after infection at a relatively low than at a higher input multiplicity (Fig. 3A).

To more precisely identify the step during the viral life cycle compromised by the mutation in BAD*sub*UL26, infected fibroblasts were assayed by Western blot for the accumulation of several viral proteins (Fig. 4A). The mutant exhibited a transient delay in the accumulation of several immediate early proteins. IE1 protein was present at a markedly reduced level at 8 h, but by 24 h, it had accumulated to wild-type levels. Immediate-early pIRS1 was detected in BADwt, not in BAD

*sub*UL26 lysates at 8 h postinfection. It accumulated to a reduced level in mutant infected cells at 24 h, and reached levels comparable to the wild type at 48 h postinfection. There was also significantly less immediate-early pTRS1 at 24 h in BAD*sub*UL26 lysates compared to the wild type, whereas at 48 h, the levels were roughly equivalent. At 24 h, BAD*sub*UL26 also accumulated slightly less pUL44, an early protein, yet by 48 h, levels of UL44 protein accumulation in mutant and wild-type virus infections were similar.

To determine if the transient reduction in IE1 protein levels displayed by BAD*sub*UL26 resulted from a reduction in IE1 mRNA, fibroblasts were infected at a multiplicity of 3 PFU/cell, and RNA accumulation was analyzed by Northern blot. As shown in Fig. 4B, reduced levels of IE1-specific mRNA had accumulated by 8 h after infection with BAD*sub*UL26 compared to the wild-type virus. By 24 h, IE1 mRNA in BAD*sub*UL26-infected cells accumulated to the same level as in wild-type-virus-infected cells. An effect of pUL26 on the accumulation of IE1 mRNA is consistent with the earlier demonstration that pUL26 activates the major immediate-early promoter when a pUL26 expression plasmid and reporter construct are transfected into cells (21).

Deletion of the UL26 ORF results in reduced intracellular levels of several tegument proteins delivered in virions. Interestingly, there seemed to be less pp28 and pp65 present in cells at 8 h after infection with BAD*sub*UL26 compared to the wild-type virus (Fig. 4A). The levels of pp28 and pp65 in mutant-infected fibroblasts appeared to reach wild-type levels by 24 and 48 h, respectively (Fig. 4A). Since both pp28 and pp65 are late proteins, their levels at 8 h should result from their delivery to newly infected cells as components of the virion's tegument. The reduced levels of these proteins at 8 h could result from a defect in the packaging of pp28 and pp65 into infectious AD*sub*UL26 particles, inefficient adsorption/entry of mutant virions into cells, or reduced stability of pp28 and pp65 once they have been delivered to the newly infected cells.

We first tested the possibility that less pp28 and pp65 was packaged into BAD*sub*UL26 particles. Mutant and wild-type virions were purified by centrifugation in a glycerol tartrate gradient, which separates infectious virions from noninfectious virus particles (4). Virion bands were removed from the gradient and normalized for total protein content, and selected virion proteins were analyzed by Western blotting (Fig. 5A). The minor capsid protein was present in similar amounts in the mutant and wild-type virion preparations, which argues that roughly equivalent numbers of mutant and wild-type virions were assayed in the experiment. The pp28 and pp65 phosphoproteins were present in the same proportion as the minor capsid protein in mutant compared to wild-type virions, which argues that they are packaged in normal quantities in the absence of pUL26.

To address the possibility that mutant virions exhibited a kinetic adsorption defect, fibroblasts were infected at a multiplicity of 3 PFU/cell for 30 min or 2 h, washed with sodium citrate to inactivate extracellular virus (8), and then analyzed by slot blotting for the delivery of viral DNA to the cell (Fig. 5B). Equivalent amounts of viral DNA had become cell associated at both times after infection with BAD*sub*UL26 or AD*wt*. The difference in input pp28 and pp65 levels does not

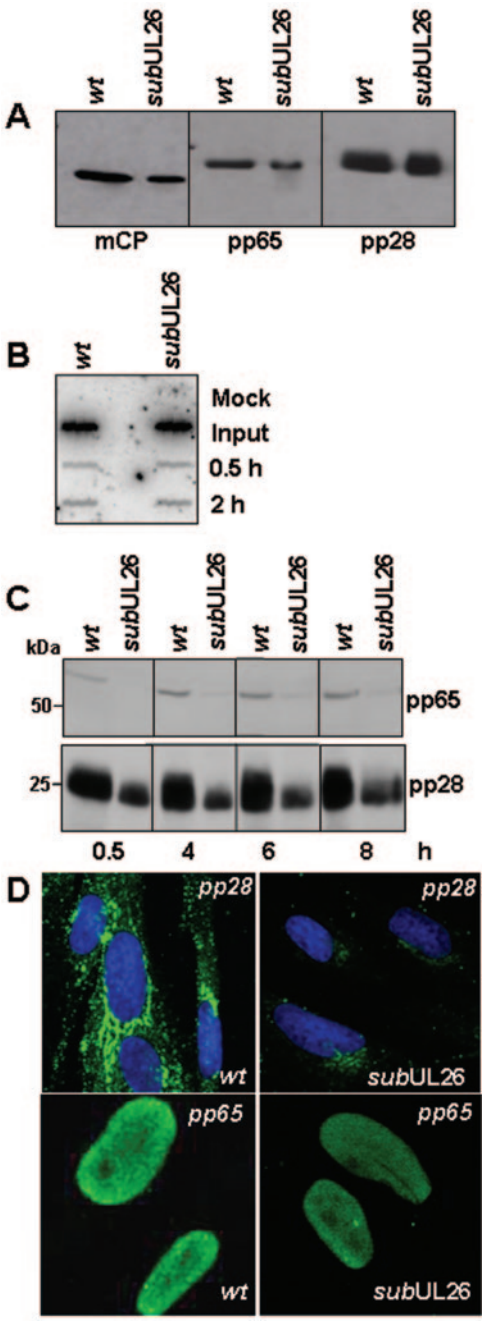

FIG. 5. Analysis of the delivery of viral proteins and DNA upon infection. (A) AD*wt* and BAD*sub*UL26 virions were purified by centrifugation in glycerol tartrate gradients. Equal amounts of virion protein were analyzed by Western blot for minor capsid protein (mCP), pp65 and pp28. (B) Replicate cultures of fibroblasts were infected at a multiplicity of 3.0 PFU/cell with AD*wt* or a BAD*sub*UL26 for 30 min or 2 h, washed with sodium citrate buffer to inactivate extra-cellular virus followed by PBS, and then harvested. Total cellular DNA along with the equivalent amount of input virus was processed for slot blot assay using an HCMV-specific probe. (C) Replicate cultures of fibroblasts were infected at a multiplicity of 3.0 with AD*wt* or BAD*sub*UL26 for 30 min, washed with sodium citrate buffer to inactivate extracellular virus, and harvested at various times. Total protein lysates were analyzed by Western blotting for pp65 and pp28 accumulation. (D) Replicate cultures of fibroblasts were infected at a multiplicity of 6.0 PFU/cell with AD*wt* or BAD*sub*UL26. Cells were fixed 4 h postinfection and processed for immunofluorescence using a pp28- or pp65-specific monoclonal antibody.

result from inefficient binding of BAD*sub*UL26 particles to the cell.

We next tested the levels of cell-associated pp65 and pp28 very early after infection of fibroblasts with mutant or wild-type virus. Adsorption was allowed to proceed for 30 min at a multiplicity of 3 PFU/cell, and cells were washed with sodium citrate to inactivate virus on the cell surface and harvested at various times thereafter. At 30 min, there was a significant decrease in the amounts of pp28 and pp65 present in cells infected with BAD*sub*UL26 compared to AD*wt* (Fig. 5C).

Mutant virions contain normal levels of the proteins (Fig. 5A) and adsorption proceeds with normal kinetics (Fig. 5B), but reduced levels of the pp28 and pp65 virion proteins are present in the cell during the early stages of infection (Fig. 5C and D). Do the reduced intracellular levels of virion proteins result from inefficient fusion and delivery of the proteins into cells or from rapid degradation of the proteins within the cells? A normal amount of viral DNA (Fig. 5B) but also reduced quantities of virion proteins (Fig. 5C) become cell associated at 30 min and 2 h after infection with the mutant. Since a fusion/entry defect would concomitantly affect the intracellular levels of both DNA and proteins, we can conclude that fusion/entry is normal and a portion of the mutant proteins is rapidly degraded after infection.

Since a portion of several BAD*sub*UL26 tegument proteins was quickly degraded after infection, it was of interest to determine if these proteins were properly localized during the early stages of infection. The localizations of pp65 and pp28 as assayed by immunofluorescence at 4 h postinfection were not discernibly different between AD*wt* and BAD*sub*UL26 (Fig. 5D), suggesting that gross localization changes are not responsible for their degradation.

BAD*sub*UL26 virions contain hypophosphorylated pp28. Although pp28 is present at roughly normal levels in BAD*sub*UL26 virions (Fig. 5A), a portion of the phosphoprotein is rapidly degraded after the tegument-associated capsid enters the newly infected cell (Fig. 5C and D). It seemed possible that the degradation could result from abnormal phosphorylation of pp28. In some but not all experiments, the pp28 delivered to cells by mutant virions appeared to migrate more rapidly than the pp28 delivered by wild-type virions (Fig. 5C), as might occur if the protein were hypophosphorylated. To explore this possibility, the proteins in gradient-purified BAD*sub*UL26 and AD*wt* virions were separated by 2-D gel electrophoresis and pp28 was identified in the patterns by Western blot assay. Multiple pp28 protein isoforms were present in wild-type virions, and several of these isoforms were present at substantially reduced levels in mutant virions (Fig. 6A), indicating that pUL26 is needed for proper posttranslational modification of virion pp28. The pp28 isoforms that were underrepresented in BAD*sub*UL26 were more slowly migrating and more acidic, suggesting that the pp28 in mutant virions is hypophosphorylated. This interpretation was confirmed by treating AD*wt* virions with phosphatase (Fig. 6B). This treatment eliminated the pp28 isoforms from the wild-type virion lysates that were underrepresented in the mutant virion lysates. These results demonstrate that pUL26 protein is required for the assembly of virions with properly phosphorylated pp28. Hypophosphorylated pp28 can be encapsidated in virions, but the protein is unstable when it is released into newly infected cells.

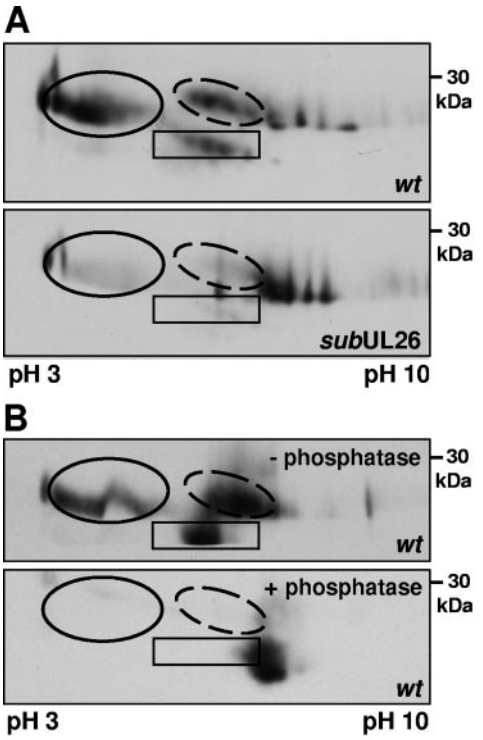

FIG. 6. Analysis of pp28 isoforms present in wild-type and pUL26 deficient mutant virions. (A) AD*wt* and BAD*sub*UL26 virions were purified by centrifugation glycerol tartrate gradients. Equal amounts of virion protein were analyzed by 2-D gel electrophoresis and immunoblotted for pp28. Altered isoforms identified by ovals and a rectangle. (B) Glycerol tartrate gradient-purified AD*wt* virions were mock treated or treated with lambda phosphatase. An equal amount of virion protein was analyzed by 2-D gel electrophoresis and immunoblotted for pp28.

DISCUSSION

Upon fusion of its envelope to the cellular membrane, the HCMV capsid and tegument are released into the cytoplasm of infected cells. As noted above, it has become increasingly clear that the proteins comprising the virion tegument perform numerous very early functions important to the establishment of a productive viral infection. Our goal in this report was to elucidate the function of the pUL26 tegument protein by analyzing the phenotype of a mutant virus.

A pUL26-deficient virus, BAD*sub*UL26, exhibited a multiplicity-dependent growth defect in fibroblasts (Fig. 3A). The mutant exhibited a significant kinetic delay after infection at a relatively low multiplicity (0.01 PFU/cell); the delay was not evident after infection at a higher multiplicity (3 PFU/cell). The mutant spread very slowly from cell to cell, taking much longer to form plaques (~1 month compared to ~2 weeks for wild-type virus [data not shown]). BAD*sub*UL26 virions exhibited a normal PFU/particle ratio. BAD*sub*UL26 and AD*wt* virion samples with equal amounts of infectivity contained the same amount of viral DNA and delivered the same amount of viral DNA to newly infected cells (Fig. 5B). A virus in which the mutation was repaired, BAD*rev*UL26, grew like wild-type virus (Fig. 3A) and pUL26 supplied in *trans* partially rescued the mutant's growth defect (Fig. 3C), arguing that the poor

growth exhibited by the mutant virus results from the loss of pUL26 function.

The earliest consequence that we observed of a pUL26 deficiency during infection involved incoming virion proteins. Two virion tegument phosphoproteins, pp28 and pp65, accumulated to reduced levels within mutant-virus-infected fibroblasts (Fig. 5C). We initially suspected that BAD*sub*UL26 virions might contain reduced levels of the two tegument proteins, but they proved to package normal quantities of pp28 and pp65 (Fig. 5A). Adsorption was found to progress with normal kinetics by monitoring the association of viral DNA with cells (Fig. 5A). Fusion and entry were judged to be normal due to the discordant relative levels of cell-associated viral DNA and tegument proteins in mutant compared to wild-type-virus-infected cells. A defect in fusion and entry would affect internalization of all virion components equally. However, the amount of cell-associated DNA was normal (Fig. 5B), whereas the levels of pp28 and pp65 tegument phosphoproteins were reduced at 30 min after infection with BAD*sub*UL26 compared to AD*wt* (Fig. 5C).

Importantly, even though BAD*sub*UL26 virions contain normal amounts of pp28 (Fig. 5A), a portion of the pp28 in mutant virions is hypophosphorylated (Fig. 6). We have not yet tested the phosphorylation states of additional tegument proteins, but others might well be affected, since pp65, like pp28, is rapidly degraded after (Fig. 5C). This leads us to propose that abnormal phosphorylation leads to the rapid degradation of pp28 and likely additional tegument proteins after BAD*sub*UL26 infection. Conceivably, the change in phosphorylation might alter the normal disassembly of the tegument, and the abnormal disassembly might lead to extensive degradation of its constituent proteins. Alternatively, hypophosphorylation might alter the interaction of pp28 with other proteins in the newly infected cell, and its failure to interact properly would lead to its destruction. To test the possibility that the proteasome mediates the degradation of a portion of the input pp28 at the start of BAD*sub*UL26 infection, fibroblasts were infected in the presence or absence of the proteasome inhibitor, MG132. The drug did not affect the levels of pp28 present after infection with mutant virus compared to wild-type virus (data not shown) suggesting that the excessive degradation of BAD *sub*UL26 virion-derived pp28 is not proteasome dependent.

Given the hypophosphorylation of pp28 in BAD*sub*UL26 virions, it is very likely that pUL26 influences the phosphorylation state of some and perhaps all HCMV tegument proteins. It might serve to direct the proper phosphorylation of tegument proteins as they are made during the late phase of infection. It is conceivable that pUL26 acts indirectly, perhaps by influencing the expression of a cellular kinase or phosphatase at the level of transcription. This notion receives support from the fact that pUL26 is localized to the nucleus during the early phase of HCMV infection (Fig. 2A and B), and earlier work has demonstrated that it contains a transcriptional activation domain (21). Alternatively, pUL26 could act directly to influence the phosphorylation of tegument proteins. It does not have a kinase active-site motif, a phosphatase active-site motif, or an ATP-binding site that we can recognize, but pUL26 could bind to a viral or cellular kinase and redirect its activity to tegument proteins, or it might bind to a phosphatase and prevent it from acting on tegument proteins. The localization of pUL26 to the juxtanuclear virion assembly domain late after infection (Fig. 2C to E) positions it to perform either of these postulated activities. It also remains possible that pUL26 does not influence the phosphorylation of tegument proteins but normally serves a gating function, excluding the encapsidation of hypophosphorylated proteins.

HCMV encodes a known protein kinase, pUL97, but we were unable to detect an interaction with pUL26 and we did not observe a change in its location after infection with the pUL26-deficient mutant (data not shown). We are currently searching for interacting cellular proteins.

Since purified BAD*sub*UL26 virions contain hypophosphorylated pp28 (Fig. 6), pUL26 must function during the late phase of infection. The timing of its action might explain the partial complementation of BAD*sub*UL26 replication by pUL26 provided in *trans* (Fig. 3C). If pUL26 normally controls phosphorylation of tegument proteins or gates their incorporation into virions during the late phase of infection, it might not effectively prevent the degradation of incoming hypophosphorylated proteins at the start of infection.

The earliest defect in the program of HCMV gene expression that we observed after infection with BAD*sub*UL26 was a marked delay in the accumulation of several immediate-early proteins: IE1, pIRS1, and pTRS1 (Fig. 4). An effect on immediate-early expression is again consistent with our observation that pUL26 localizes to the nucleus early during infection (Fig. 2A and B) and with a previous report that domain within pUL26 can upregulate major immediate-early promoter activity in transient transfection assays (21). However, pUL26 could well act indirectly to influence expression of the major immediate-early gene product, given our demonstration that it stabilizes the pp28 and pp65 tegument phosphoproteins (Fig. 4A and 5C). For example, pUL26 might also stabilize the UL82-coded pp71 tegument phosphoprotein, which activates transcription in transfection assays (13) and enhances the accumulation of several immediate-early mRNAs within infected cells (4).

We nevertheless tested the possibility that reduced IE1 expression is responsible for the BAD*sub*UL26 growth defect. Since the inhibition of histone deacetylase (HDAC) activity can rescue the growth of an IE1-null mutant (15), we reasoned that treatment with an HDAC inhibitor would rescue BAD *sub*UL26 replication if its replication defect was ultimately due to reduced IE1 expression. However, trichostatin A, an HDAC inhibitor that compensates for the loss of IE1 activity, had no effect on BAD*sub*UL26 replication (data not shown). Not surprisingly, then, an effect on IE1 activity is not solely responsible for the BAD*sub*UL26 replication defect.

In conclusion, a pUL26-deficient mutant produces virions with hypophosphorylated pp28 protein, and a portion of this virion protein is rapidly degraded at the start of infection. We propose that pUL26 regulates the phosphorylation of several if not all tegument proteins, and we speculate that proper phosphorylation is necessary for their normal function and stability.

ACKNOWLEDGMENTS

We thank Thomas Stamminger (Universitat Zurich) for the generous gift of rabbit polyclonal anti-pUL26 antibody and P. Robinson (Princeton University) for assistance in the production of mouse monoclonal anti-pUL26.

This work was supported by a grant from the NIH (CA82396), and J.M. was supported by a postdoctoral fellowship from the American Cancer Society.

REFERENCES

1. **Abate, D. A., S. Watanabe, and E. S. Mocarski.** 2004. Major human cytomegalovirus structural protein pp65 (ppUL83) prevents interferon response factor 3 activation in the interferon response. J. Virol. **78:**10995–11006.
2. **Anderson, M. L. M.** 1999. Nucleic acid hybridization. Springer, New York, N.Y.
3. **Baldick, C. J., Jr., and T. Shenk.** 1996. Proteins associated with purified human cytomegalovirus particles. J. Virol. **70:**6097–6105.
4. **Bresnahan, W. A., and T. E. Shenk.** 2000. UL82 virion protein activates expression of immediate early viral genes in human cytomegalovirus-infected cells. Proc. Natl. Acad. Sci. USA **97:**14506–14511.
5. **Browne, E. P., and T. Shenk.** 2003. Human cytomegalovirus UL83-coded pp65 virion protein inhibits antiviral gene expression in infected cells. Proc. Natl. Acad. Sci. USA **100:**11439–11444.
6. **Child, S. J., M. Hakki, K. L. De Niro, and A. P. Geballe.** 2004. Evasion of cellular antiviral responses by human cytomegalovirus TRS1 and IRS1. J. Virol. **78:**197–205.
7. **Dunn, W., C. Chou, H. Li, R. Hai, D. Patterson, V. Stolc, H. Zhu, and F. Liu.** 2003. Functional profiling of a human cytomegalovirus genome. Proc. Natl. Acad. Sci. USA **100:**14223–14228.
8. **Feire, A. L., H. Koss, and T. Compton.** 2004. Cellular integrins function as entry receptors for human cytomegalovirus via a highly conserved disintegrin-like domain. Proc. Natl. Acad. Sci. USA **101:**15470–15475.
9. **Gerna, G., F. Baldanti, and M. G. Revello.** 2004. Pathogenesis of human cytomegalovirus infection and cellular targets. Hum. Immunol. **65:**381–386.
10. **Kalejta, R. F., J. T. Bechtel, and T. Shenk.** 2003. Human cytomegalovirus pp71 stimulates cell cycle progression by inducing the proteasome-dependent degradation of the retinoblastoma family of tumor suppressors. Mol. Cell. Biol. **23:**1885–1895.
11. **Kinsella, T. M., and G. P. Nolan.** 1996. Episomal vectors rapidly and stably produce high-titer recombinant retrovirus. Hum. Gene Ther. **7:**1405–1413.
12. **Kulesza, C. A., and T. Shenk.** 2004. Human cytomegalovirus 5-kilobase immediate-early RNA is a stable intron. J. Virol. **78:**13182–13189.
13. **Liu, B., and M. F. Stinski.** 1992. Human cytomegalovirus contains a tegument protein that enhances transcription from promoters with upstream ATF and AP-1 *cis*-acting elements. J. Virol. **66:**4434–4444.
14. **Lu, M., and T. Shenk.** 1999. Human cytomegalovirus UL69 protein induces cells to accumulate in G_1 phase of the cell cycle. J. Virol. **73:**676–683.
15. **Nevels, M., C. Paulus, and T. Shenk.** 2004. Human cytomegalovirus immediate-early 1 protein facilitates viral replication by antagonizing histone deacetylation. Proc. Natl. Acad. Sci. USA **101:**17234–17239.
16. **Nowak, B., C. Sullivan, P. Sarnow, R. Thomas, F. Bricout, J. C. Nicolas, B. Fleckenstein, and A. J. Levine.** 1984. Characterization of monoclonal antibodies and polyclonal immune sera directed against human cytomegalovirus virion proteins. Virology **132:**325–338.
17. **Romanowski, M. J., and T. Shenk.** 1997. Characterization of the human cytomegalovirus *irs1* and *trs1* genes: a second immediate-early transcription unit within *irs1* whose product antagonizes transcriptional activation. J. Virol. **71:**1485–1496.
18. **Rowe, W. P., J. W. Hartley, S. Waterman, H. C. Turner, and R. J. Huebner.** 1956. Cytopathogenic agent resembling human salivary gland virus recovered from tissue cultures of human adenoids. Proc. Soc. Exp. Biol. Med. **92:**418–424.
19. **Sanchez, V., K. D. Greis, E. Sztul, and W. J. Britt.** 2000. Accumulation of virion tegument and envelope proteins in a stable cytoplasmic compartment during human cytomegalovirus replication: characterization of a potential site of virus assembly. J. Virol. **74:**975–986.
20. **Silva, M. C., Q. C. Yu, L. Enquist, and T. Shenk.** 2003. Human cytomegalovirus UL99-encoded pp28 is required for the cytoplasmic envelopment of tegument-associated capsids. J. Virol. **77:**10594–10605.
21. **Stamminger, T., M. Gstaiger, K. Weinzierl, K. Lorz, M. Winkler, and W. Schaffner.** 2002. Open reading frame UL26 of human cytomegalovirus encodes a novel tegument protein that contains a strong transcriptional activation domain. J. Virol. **76:**4836–4847.
22. **Varnum, S. M., D. N. Streblow, M. E. Monroe, P. Smith, K. J. Auberry, L. Pasa-Tolic, D. Wang, D. G. Camp II, K. Rodland, S. Wiley, W. Britt, T. Shenk, R. D. Smith, and J. A. Nelson.** 2004. Identification of proteins in human cytomegalovirus (HCMV) particles: the HCMV proteome. J. Virol. **78:**10960–10966.
23. **Yu, D., M. C. Silva, and T. Shenk.** 2003. Functional map of human cytomegalovirus AD169 defined by global mutational analysis. Proc. Natl. Acad. Sci. USA **100:**12396–12401.
24. **Yu, D., G. A. Smith, L. W. Enquist, and T. Shenk.** 2002. Construction of a self-excisable bacterial artificial chromosome containing the human cytomegalovirus genome and mutagenesis of the diploid TRL/IRL13 gene. J. Virol. **76:**2316–2328.